Archives of Mechanics • Archiwum Mechaniki Stosowanej • 28, 3, pp. 531–547, Warszawa 1976

The effective elastic response of randomly oriented polycrystalline solids in tension

J. W. PROVAN and D. R. AXELRAD (MONTREAL)

THE present paper represents one of our first attempts to apply the probabilistic micromechanics theory, albeit in its elastic format, to actual polycrystalline solids in the form of pure copper and aluminium constrained in a simple but realistic boundary value configuration. In doing so it is observed that all of the previously introduced experimental material, kinematic and stress concepts of the micromechanics theory pertaining to the elastic deformation of polycrystalline materials have been utilized and, for the first time in most instances, are numerically evaluated for the two materials in question. In particular, the actual numerical determination of microstress distributions in the case of uniaxially stressed specimens has represented one of the primary goals of micromechanics since its inception.

Praca niniejsza stanowi jedną z pierwszych prób zastosowania probabilistycznej teorii mikromechaniki w zakresie sprężystym do aktualnych polikrystalicznych ciał stałych takich jak czysta miedź i aluminium, ograniczonych więzami przez prostą lecz realną konfigurację brzegu. Zauważono przy tym, że wszystkie wyprowadzone poprzednio koncepcje dotyczące eksperymentu, materiału, kinetyki i naprężenia w teorii mikromechaniki, odnoszące się do deformacji sprężystej materiałów polikrystalicznych, zostały wykorzystane i po raz pierwszy zostały wyznaczane numerycznie dla wyżej wspomnianych dwóch materiałów. W szczególności wprowadzone określenie numeryczne rozkładu mikronaprężeń w przypadku jednoosiowych naprężanych próbek stanowi jeden z głównych celów mikromechaniki.

Настоящая работа составляет одну из первых попыткок применения пробабилистической теории микромеханики, но только в упругой области, к актуальным поликристаллическим твердым телам, таким как чистая медь и алюминий, ограниченных связями простой, но реальной конфигурации границы. При этом констатируется, что все введенные раньше концепции эксперимента, материала, кинетики и напряжения в теории микромеханики, относящиеся к упругой деформации поликристаллических материалов, были использованы и впервые численно определены для выше упомянутых двух материалов. В частности данное численное определение распределения микронапряжений, в случае односно напряженных образцов, составляло одну из главных целей микромеханики от времен ее возникновения.

1. Introduction

THE description of the mechanical response of polycrystalline solids has been the objective of many theoreticians working in the general field of continuum and applied mechanics. The question naturally arises as to whether it is possible to bridge the gap between these theories and the information constantly being made available concerning the mechanical responses of such solids on their atomic and molecular level. Basically, this was one of the goals of micromechanics as expressed in the 1972 lecture series [1](1) and recently more fully described in the monograph by D. R. AXELRAD [2]. Since that time we have

(1) Bracketed numbers denote references list at the end of this paper.

made progress towards answering some of the hypotheses proposed in [1] and the present work constitutes the first time that it has been possible to apply micromechanics theory to real polycrystalline solids and to obtain quantitative values for the large number of variables involved. In our opinion the effort involved has been vindicated by the results obtained.

Micromechanics theory considers that the kinematic parameters involved in the deformation process are random variables in the elastic case and stochastic processes in the irreversible case. Restricting our attention to the elastic response, the polycrystalline random kinematic variables are defined and reviewed in Table 1. The indicated references may be consulted for more details.

Table 1. Kinematic random variables

Symbol	Main Ref.	Interpretation
$\mathbf{x} : x_i \sim (x_1, x_2, x_3)$	[4] Fig. 1	External coordinate frame: location of any point.
${}^{\alpha}\mathbf{y} : {}^{\alpha}y_\gamma \sim ({}^{\alpha}y_1, {}^{\alpha}y_2, {}^{\alpha}y_3)$	[4]	Internal coordinate frame of α^{th} microelement: location of any point in α.
${}^{\alpha}\mathbf{r} : {}^{\alpha}r_i \sim ({}^{\alpha}r_1, {}^{\alpha}r_2, {}^{\alpha}r_3)$	[4]	Location of center of α with regard to x_i.
${}^{\alpha\beta}\boldsymbol{\zeta}_a \sim ({}^{\alpha}\mathbf{n} \times {}^{\alpha\beta}\boldsymbol{\lambda}, {}^{\alpha}\mathbf{n}, {}^{\alpha\beta}\boldsymbol{\lambda})$	[3] Fig. 1	Grain boundary coordinate frame.
${}^{\alpha}\mathbf{n} \sim ({}^{\alpha}n_1, {}^{\alpha}n_2, 0)$	[3] Fig. 1	Unit normal to grain boundary of α with regard to x_i.
${}^{\alpha\beta}\boldsymbol{\lambda} \sim (0, 0, 1)$	[3] Fig. 1	Direction about which a rotation of θ^0 superimposes the crystallographic axes of the α and β contiguous microelements with regard to x_i.
θ^0	[4]	Mismatch rotation angle.
${}^{\alpha\beta}\mathbf{d} : {}^{\alpha\beta}d_a \sim ({}^{\alpha\beta}d_1, {}^{\alpha\beta}d_2, {}^{\alpha\beta}d_3)$	[4]	Relative g.b. displacement w.r.t. ${}^{\alpha\beta}\boldsymbol{\zeta}_a$.
${}^{\alpha\beta}\boldsymbol{\delta} : {}^{\alpha\beta}\delta_a \sim ({}^{\alpha\beta}d_1, {}^{\alpha\beta}d_2 + \Delta, {}^{\alpha\beta}d_3)$	[4]	Deformed counterpart of $\boldsymbol{\Delta}$.
Undeformed counterparts of above are indicated by their corresponding majuscules		
$\boldsymbol{\Delta} : \Delta_a \sim (0, \Delta, 0)$	[4]	Grain boundary thickness w.r.t. ${}^{\alpha\beta}\boldsymbol{\zeta}_a$.
${}^{\alpha}\mathbf{w} = {}^{\alpha}\mathbf{y} - {}^{\alpha}\mathbf{y} : {}^{\alpha}w_\gamma$	[4]	Displacement of point within α.
${}^{\alpha}\mathbf{e} : {}^{\alpha}e_{\delta\lambda} = \frac{1}{2}({}^{\alpha}w_{\delta,\lambda} + {}^{\alpha}w_{\lambda,\delta})$	[4]	Linear microstrain in α.
${}^{\alpha\beta}\mathbf{e} : {}^{\alpha\beta}e_{ab} = \frac{1}{2}({}^{\alpha\beta}d_{a,b} + {}^{\alpha\beta}d_{b,a})$	[3] [4]	Linear microstrain in grain boundary.

By introducing the three measuring scales, denoted by, micro-, meso-, and macro- the microkinematic parameters listed in this table have been transformed into probabilistic density and distribution functions and into mean values and variances of the parameters involved. These two quantities are all that are required for a complete description of any, particular kinematic probability density function under the micromechanic assumption

that all such distributions are Gaussian. An explicit description of the strains discussed above and involved in the boundary value problem developed in this paper, based upon the experimental holographic interferometric results described by AXELRAD and KALOUSEK [6] and KALOUSEK [7], is presented in Sect. 3.

The third basic micromechanic concept is that of the existence of a material operator ${}^{M}\mathfrak{M}$ which takes the place of the conventional constitutive relations and is developed, not from the classical macroscopic response of materials but from studies of their atomic, molecular and microscopic mechanical behaviour. In other words, although the operational characteristics of conventional constitutive relations and ${}^{M}\mathfrak{M}$ are largely the same they are numerically specified on the basis of entirely different experimental observations. Hence, prediction of the influence of theoretical microstructure changes on the macroresponse characteristics of the material in question thereby becomes feasible. The material operator ${}^{M}\mathfrak{M}$ for the elastic response of polycrystalline solids has been formulated in detail in previous publications and its parameters and notations are simply listed in Table 2

Table 2. Material operator coefficients

Symbol	Main Ref.	Interpretation
${}^{M}\mathfrak{m} = [(1-\varkappa)\mathsf{H}^{-1}+\varkappa(\mathbf{\Lambda}\mathsf{E})^{-1}]^{-1}{}^{M}\mathfrak{m}_{ijkl}$:	[3]	Elastic material operator for polycrystalline solids.
H:H_{ijkl}; H^{-1}:H^{-1}_{ijkl}	[3] Table 5	Material operators for single microelements.
${}^{\alpha\beta}\zeta_a = {}^{\alpha\beta}\alpha_{ja}x_i$	Eq. (5, 6)	Direction cosines.
${}^{\alpha\beta}\mathbf{\Lambda}$:${}^{\alpha\beta}\alpha_{ia}{}^{\alpha\beta}\alpha_{jb}{}^{\alpha\beta}\alpha_{kc}{}^{\alpha\beta}\alpha_{ld}$	Sect. 5	Grain boundary coordinate transfer operator.
$\mathbf{\Lambda} = \langle{}^{\alpha\beta}\mathbf{\Lambda}\rangle = \int {}^{\alpha\beta}\mathbf{\Lambda}d\mathscr{P}n$	Sect. 5	First statistical moment of ${}^{\alpha\beta}\mathbf{\Lambda}$.
${}^{\alpha\beta}\mathsf{E}$:${}^{\alpha\beta}E_{abcd}$; ${}^{\alpha\beta}\mathsf{E}^{-1} = {}^{\alpha\beta}E^{-1}_{abcd}$	Sect. 5	Material operators for grain boundary.
$\mathsf{E} = \langle{}^{\alpha\beta}\mathsf{E}\rangle = \int {}^{\alpha\beta}\mathsf{E}d\mathscr{P}\theta$	Sect. 5	First statistical moment of ${}^{\alpha\beta}\mathsf{E}$.
$\varkappa$	[3]	Statistical frequency of g.b. material.
$\eta = \frac{2}{3\pi}G(1-\nu)l^2\sigma\varrho_d$	[3], [8] Table 4	The influence of inactivated Frank-Read dislocation sources on the elastic response of single microelements.
G, ν		Shear modulus, Poisson's ratio.
l	[8]	Characteristic distance between pinning points of an edge dislocation.
$\sigma\varrho_d$	[8]	The mobile dislocation density.
${}^{\alpha\beta}A_a \sim ({}^{\alpha\beta}A_1, {}^{\alpha\beta}A_2, {}^{\alpha\beta}A_3)$	[10] Sect. 5	G.b. elastic responses in ζ_a directions.
$A_a = \langle{}^{\alpha\beta}A_a\rangle = \int {}^{\alpha\beta}Ad\mathscr{P}\theta$	Table 5	First statistical moment of ${}^{\alpha\beta}A_a$.

where again the appropriate references are noted. Quantitative values for the elastic response of the microelements or grains of pure polycrystalline copper and aluminium, based upon a dislocation model [8] involving the inactivated Frank-Read source, are evaluated in Sect. 4, while the summarized results of recent grain boundary studies [9, 10] are presented in Sect. 5. Section 6 combines the results of these two studies, as

indicated in Table 2, in order to quantitatively formulate expressions for the material operator for pure polycrystalline copper and aluminium.

Once the explicit expressions for the material operator are available it is no problem to combine them with the experimentally obtained strain distributions of Sect. 3 to obtain expressions for the density functions of microstresses in specimens of copper and aluminium loaded as described in Sect. 2. This part of the work is described in Sect. 7 where conclusions are also drawn.

Until recently, the elastic response was studied solely in order to check the validity of the basic micromechanic hypotheses before delving into a quantitative description of an actual irreversible response, such as creep or fatigue, of a real material. As discussed in [3 and 5], however, it now appears that at least the probabilistic form of the secondary creep and linear viscoelastic responses of polycrystalline solids may be completely described by a knowledge of the elastic response and a so called "kinematic transition probability matrix", thereby placing additional emphasis on the explicit knowledge of the reversible response of such materials. An extension of this concept to the transition zone between the purely elastic response and the irreversible response described by a time dependent transition probability matrix constitutes an accompanying presentation at this symposium [11].

Finally, in what follows, miniscules denote deformed components of their undeformed majuscule counterparts and direct notation is utilized throughout the development. For clarification, Cartesian tensor notation is occasionally reverted to with Latin indices i, j, k, l, indicating reference to the external coordinate frame, Latin indices a, b, c, d, refer to grain boundary coordinates, while Greek indices indicate the interior coordinate system of the individual microelement.

2. Choice of boundary value problem configuration

To the knowledge of the authors the only available data for the determination of explicit strain distributions, $\mathscr{P}^{\varepsilon}$, is the work of AXELRAD and KALOUSEK [6, 7]. They used a two-phase material consisting of pure aluminium monocrystals embedded in an epoxy resin matrix and established distribution histograms for two translations and one rotation by a combined holographic interferometry and X-ray back-reflection Laué technique. Their experimental results, as utilized in the following section, are limited to the uniaxial tension of the two-phase model with the $2\times2\times2\ \mathrm{mm}^3$ aluminium monocrystals preoriented such that their [001] crystallographic axis, with reference to Fig. 1, is always in the x_3-direction and the normals to their epoxy embedded surfaces are uniformly distributed in the x_1, x_2-plane. This experimental configuration, along with the computational simplifications brought about, has constrained the discussion to polycrystalline specimens of copper and aluminium with the dimensions, orientations and coordinates as indicated in Fig. 1. The three particular probability measures $\mathscr{P}^{\eta}$, obtained from $\mathscr{P}^{\phi} = \frac{\phi}{\pi}\{H(\phi)-H(\phi-\pi)\}$, $\mathscr{P}^{\phi} = \delta(\phi)$ and $\mathscr{P}^{\phi} = \delta\left(\phi-\frac{\pi}{2}\right)$ are examined throughout this paper in order to discuss the limiting cases of the influence of crystallographic

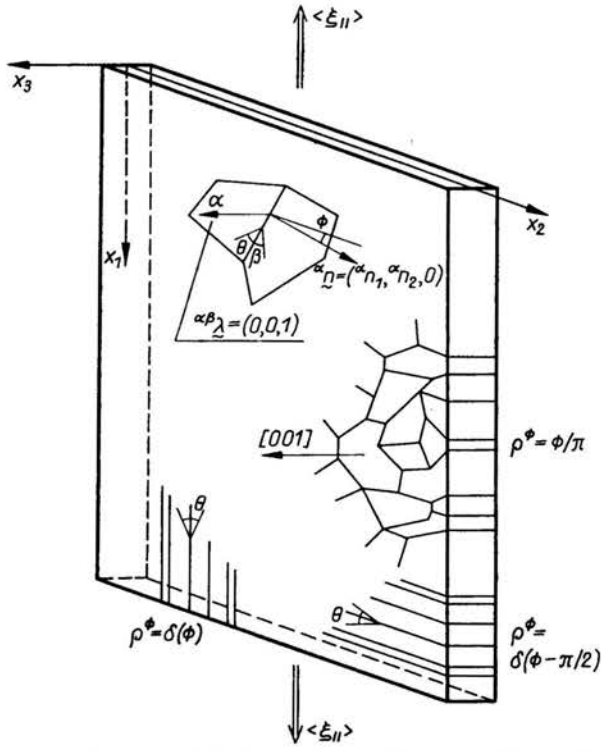

FIG. 1. Scheme of idealized polycrystalline material sample.

grain boundary orientations on the overall mechanical response and microstress distributions in polycrystalline copper and aluminium.

Furthermore, in connection with topics discussed in Sect. 5 of this paper, only symmetric tilt boundaries with mismatch orientation angles of $\theta = 22.6^{\circ}$, 28.1°, 31.9°, 36.9° and 53.1° have been studied in detail for copper and aluminium in Refs. [9 and 10]. Hence, for both the materials and for the three distributions of grain boundary normals introduced above, the distribution of θ is chosen to reflect this limitation. Due to both the large number of crystallographic symmetries in both copper and aluminium and to the marked tendency of crystals to unite with coincidence mismatch orientations [14], it is felt that the five angles chosen are sufficient to describe a large proportion of grain boundaries in polycrystalline copper and aluminium.

3. Distributions of strains

Micromechanics theory postulates the existence not of a deterministic strain field but of a probablistic one. In order to obtain distributions for the three strains e_{11}, e_{22} and e_{12}, the basic two-dimensional displacement and rotation histograms, obtained by the combined holographic and X-ray technique introduced in [6] and presented in [3 and 7], are utilized in this section. We are, of course, aware of the limitations of the proposed method of obtaining strain measurements and of the results obtained but until better

measurements are available the strain measurement histograms about to be developed are considered to be sufficient both to illustrate the use of the micromechanics theory and to draw some interesting conclusions.

As mentioned in Sect. 2 the displacement results were obtained for a two-phase model consisting of 147 monocrystals of aluminium embedded in an epoxy resin matrix. By measuring the undeformed distance between the geometric center of neighbouring crystals and by taking the difference between their displacements measured by holographic interferometry, strain approximations were determined by appropriate divisions of the latter by the former. Simple calculations led to the means and variances listed in Table 3 for

Table 3. Strain means and standard deviations

	e_{11}	e_{22}	e_{12}
$\langle \mathbf{e} \rangle$	0.445×10^{-3}	0.0	0.0
$\sigma_e = \sqrt{V_e}$	0.2×10^{-3}	0.25×10^{-3}	0.3×10^{-3}

an average stress level of $\langle \xi_{11} \rangle = 2.5 \times 10^3$ dynes/cm^2. This low stress level was chosen to ensure that the aluminium monocrystals were stressed within their elastic limit.

In Sect. 7, the microstrain means and variances of Table 3 are utilized to determine microstress distributions in both polycrystalline aluminium and copper. This is of course incorrect since the experimental two-phase model used in determining the Table 3 information is not the same as either pure polycrystalline copper or aluminium. However, as stated previously they are the only results at present available to us for utilization in determining the validity of the micromechanics approach. It is hoped that the results expressed in this paper will motivate other researchers to begin to investigate non-deterministic, rather than phenomenological, strain fields developed in externally loaded polycrystalline specimens.

4. Material operator—grain interior response

Effectively, polycrystalline solids are considered to consist of two distinct zones; the separate crystals and the grain boundary between contiguous grains. The first zone, consisting of the grains themselves, have the kinematic and strain random variables listed in Table 1 and the constitutive response given in Table 2. Using the appropriate sources listed, Table 4 gives the numerical values of both H_{ijkl} and H^{-1}_{ijkl} for copper and aluminium as deduced from the constitutive relations shown.

5. Material operator—constitutive relations for grain boundaries in copper and aluminium

Computer simulations of the mechanical response of symmetric tilt grain boundaries with crystallographic mismatch angles of $\theta = 22.6^\circ$, 28.1°, 31.9°, 36.9°, and 53.1° in pure copper and aluminium have recently been presented by BAMIRO and PROVAN [9, 10].

Table 4. The mechanical response of copper and aluminium monocrystals

Basic Equations			Main Ref.
$\mathsf{H}: H_{ijkl} = \frac{2G^2}{G+4\eta}\delta_{ik}\delta_{jl} + \frac{2G[3G\nu+4\eta(1+\nu)]}{3(1-2\nu)(G+4\eta)}\delta_{ij}\delta_{kl}$			[3] Table 2
$\mathsf{H}^{-1}: H^{-1}_{ijkl} = \frac{G+4\eta}{2G^2}\delta_{ik}\delta_{jl} - \frac{3G\nu+4\eta(1+\nu)}{6G^2(1+\nu)}\delta_{ij}\delta_{kl}$			[3] Table 2
Parameter	Copper	Aluminium	
G	9.5×10^{11} dynes/cm^2	2.86×10^{11} dynes/cm^2	[15], [16]
ν	0.324	0.347	[12]
σ_{ϱ_d}	10^7 cm/cm^3	10^7 cm/cm^3	[13]
l	3×10^{-5} cm	3×10^{-5} cm	[12]
η	12.26×10^8 dynes/cm^2	3.57×10^8 dynes/cm^2	[8] Table 2
H	$18.9\times10^{11}\delta_{ik}\delta_{jl}+17.52\times10^{11}\delta_{ij}\delta_{kl}$ dynes/cm^2	$5.69\times10^{11}\delta_{ik}\delta_{jl}+6.497\times10^{11}\delta_{ij}\delta_{kl}$ dynes/cm^2	
H^{-1}	$5.29\times10^{-13}\delta_{jk}\delta_{jl}-1.297\times10^{-13}\delta_{ij}\delta_{kl}$ cm^2/dyne	$17.6\times10^{-13}\delta_{ik}\delta_{jl}-4.533\times10^{-13}\delta_{ij}\delta_{kl}$ cm^2/dyne	

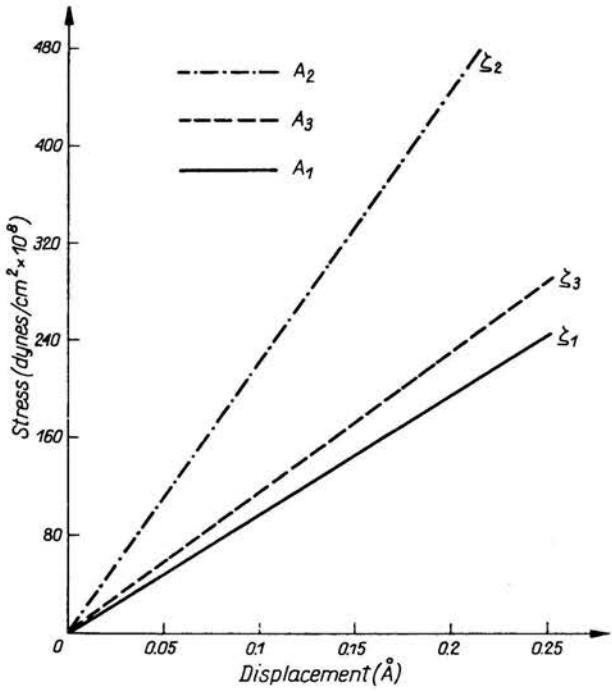

FIG. 2. Average stress-displacement curves for copper boundaries.

The chief motivation behind the work involved in the preparation of these two reports, which are mainly of interest to researchers in the field of computer simulated grain boundary configurations and energies, has been the micromechanic desire, first expressed in [1 and 4], for quantitative information concerning the mechanical response of grain boundaries in polycrystalline solids. This information was required in order to complete the numerical knowledge of the parameters involved in the material operator ${}^{M}\mathfrak{M}$ as expressed in Table 2. The results are reproduced in Table 5. Figure 2 compares, with

Table 5. Grain boundary response at 673°K in copper and aluminium

	Copper		dynes / cm² Å	Aluminium		dynes / cm² Å
θ^0	${}^{\alpha\beta}A_1$ ($\times 10^8$)	${}^{\alpha\beta}A_2$ ($\times 10^8$)	${}^{\alpha\beta}A_3$ ($\times 10^8$)	${}^{\alpha\beta}A_1$ ($\times 10^8$)	${}^{\alpha\beta}A_2$ ($\times 10^8$)	${}^{\alpha\beta}A_3$ ($\times 10^8$)
22.6	490	1376	606	600	1712	464
28.1	300	1414	580	540	984	808
31.9	134	2048	472	2064	2496	1816
36.9	454	338	358	120	600	890
53.1	3508	5988	3760	752	642	920
	A_1 ($\times 10^8$)	A_2 ($\times 10^8$)	A_3 ($\times 10^8$)	A_1 ($\times 10^8$)	A_2 ($\times 10^8$)	A_3 ($\times 10^8$)
$\int {}^{\alpha\beta}A_a d\mathscr{P}^\theta$	977.2	2232.8	1155.2	815.2	1286.8	979.6

respect to the coordinate directions ζ_a, $a = 1, 2, 3$, the slopes and hence the relative mechanical strengths of symmetric tilt boundaries in copper. These slopes represent the moduli, A_a, with respect to displacements in the ζ_a directions.

The grain boundary constitutive relations as a function of material, mismatch orientation angle, θ, and temperature are obtained from the grain boundary strain tensor derived in [3] and listed for convenience in Table 1, namely:

$$(5.1) \qquad {}^{\alpha\beta}e_{ab} \sim 1/2 \begin{bmatrix} . & {}^{\alpha\beta}d_1/\Delta & . \\ {}^{\alpha\beta}d_1/\Delta & 2^{\alpha\beta}d_2/\Delta & {}^{\alpha\beta}d_3/\Delta \\ . & {}^{\alpha\beta}d_2/\Delta & . \end{bmatrix},$$

the grain boundary computer simulated stress-displacement relations:

$$(5.2) \qquad {}^{\alpha\beta}\xi_{ab} \sim \begin{bmatrix} . & {}^{\alpha\beta}A_1{}^{\alpha\beta}d_1 & . \\ {}^{\alpha\beta}A_1{}^{\alpha\beta}d_1 & {}^{\alpha\beta}A_2{}^{\alpha\beta}d_2 & {}^{\alpha\beta}A_3{}^{\alpha\beta}d_3 \\ . & {}^{\alpha\beta}A_3{}^{\alpha\beta}d_3 & . \end{bmatrix}$$

and the assumption that the grain boundary response to "in plane" tensions and shears is identical to that of the bulk isotropic crystalline material, i.e.:

$$(5.3) \qquad \begin{aligned} {}^{\alpha\beta}\xi_{11} &= H_{1111}{}^{\alpha\beta}e_{11} + H_{1133}{}^{\alpha\beta}e_{33}, \\ {}^{\alpha\beta}\xi_{33} &= H_{1111}{}^{\alpha\beta}e_{11} + H_{1133}{}^{\alpha\beta}e_{33}, \\ {}^{\alpha\beta}\xi_{13} &= H_{1313}{}^{\alpha\beta}e_{13}. \end{aligned}$$

Hence, the grain boundary constitutive relation can be written as:

$$^{\alpha\beta}\xi_{ab} = {}^{\alpha\beta}E_{abcd}\,{}^{\alpha\beta}e_{cd}, \tag{5.4}$$

where its material matrix is given by:

$$^{\alpha\beta}\mathbf{E}:{}^{\alpha\beta}E_{abcd} \sim \begin{bmatrix} H_{1111} & 0 & H_{1133} & 0 & 0 & 0 \\ & {}^{\alpha\beta}A_2\Delta & 0 & 0 & 0 & 0 \\ & & H_{3333} & 0 & 0 & 0 \\ & & & 2^{\alpha\beta}A_3\Delta & 0 & 0 \\ & & & & H_{1313} & 0 \\ & & & & & 2^{\alpha\beta}A_1\Delta \end{bmatrix} \tag{5.5}$$

Upon referring the local grain boundary coordinates $^{\alpha\beta}\zeta_a$ to the external coordinate system x_i by:

$$^{\alpha\beta}\zeta_a = {}^{\alpha\beta}\alpha_{ia}x_i \tag{5.6}$$

the constitutive relation (5.4) may be written in terms of the external coordinates as:

$$^{\alpha\beta}\boldsymbol{\xi} = {}^{\alpha\beta}\boldsymbol{\Lambda}\,{}^{\alpha\beta}\mathbf{E}\,{}^{\alpha\beta}\mathbf{e}:{}^{\alpha\beta}\xi_{ij} = {}^{\alpha\beta}\alpha_{ia}\,{}^{\alpha\beta}\alpha_{jb}\,{}^{\alpha\beta}\alpha_{kc}\,{}^{\alpha\beta}\alpha_{ld}\,{}^{\alpha\beta}E_{abcd}\,{}^{\alpha\beta}e_{kl}. \tag{5.7}$$

Restricting, now, attention to the particular boundary value configuration introduced in Sect. 2 the direction cosines, $^{\alpha\beta}\alpha_{ia}$, expressed in (5.6) become in terms of angle ϕ indicated in Fig. 1:

$$^{\alpha\beta}\alpha_{ia} \sim \begin{bmatrix} \cos{}^{\alpha\beta}\phi & \sin{}^{\alpha\beta}\phi & 0 \\ -\sin{}^{\alpha\beta}\phi & \cos{}^{\alpha\beta}\phi & 0 \\ 0 & 0 & 1 \end{bmatrix}. \tag{5.8}$$

With this particular choice of grain boundary orientation and the strain field introduced in Sect. 3, the general expression (5.7) reduces to the following three equations:

$$\begin{aligned} (5.9)_1 \quad \frac{^{\alpha\beta}\xi_{11}}{\Delta} &= \left\{{}^{\alpha\beta}C_1\,{}^{\alpha\beta}A_2 + {}^{\alpha\beta}C_5\frac{H_{1111}}{\Delta} + 4^{\alpha\beta}C_3\,{}^{\alpha\beta}A_1\right\}{}^{\alpha\beta}e_{11} \\ &\quad + 2\{{}^{\alpha\beta}C_2\,{}^{\alpha\beta}A_2 + 2({}^{\alpha\beta}C_4 - {}^{\alpha\beta}C_2)^{\alpha\beta}A\}{}^{\alpha\beta}e_{12} + {}^{\alpha\beta}C_3\{{}^{\alpha\beta}A_2 + H_{1111}/\Delta - 4^{\alpha\beta}A_1\}{}^{\alpha\beta}e_{22}; \\ (5.9)_2 \quad \frac{^{\alpha\beta}\xi_{12}}{\Delta} &= \left\{{}^{\alpha\beta}C_2\,{}^{\alpha\beta}A_2 - {}^{\alpha\beta}C_4\frac{H_{1111}}{\Delta} + 2({}^{\alpha\beta}C_4 - {}^{\alpha\beta}C_2)^{\alpha\beta}A_1\right\}{}^{\alpha\beta}e_{11} \\ &\quad + \left\{{}^{\alpha\beta}C_3\,{}^{\alpha\beta}A_2 + {}^{\alpha\beta}C_3\frac{H_{1111}}{\Delta} + 2({}^{\alpha\beta}C_5 - 2^{\alpha\beta}C_3 + {}^{\alpha\beta}C_1)^{\alpha\beta}A_1\right\}{}^{\alpha\beta}e_{12} \\ &\quad \left\{{}^{\alpha\beta}C_4\,{}^{\alpha\beta}A_2 - {}^{\alpha\beta}C_2\frac{H_{1111}}{\Delta} + 2({}^{\alpha\beta}C_2 - {}^{\alpha\beta}C_4)^{\alpha\beta}A_1\right\}{}^{\alpha\beta}e_{22}; \\ (5.9)_3 \quad \frac{^{\alpha\beta}\xi_{22}}{\Delta} &= \left\{{}^{\alpha\beta}C_3\,{}^{\alpha\beta}A_2 + {}^{\alpha\beta}C_3\frac{H_{1111}}{\Delta} - 4^{\alpha\beta}C_3\,{}^{\alpha\beta}A_1\right\}{}^{\alpha\beta}e_{11} \\ &\quad + 2\{{}^{\alpha\beta}C_4\,{}^{\alpha\beta}A_2 + 2({}^{\alpha\beta}C_2 - {}^{\alpha\beta}C_4)^{\alpha\beta}A_1\}{}^{\alpha\beta}e_{12} + \left\{{}^{\alpha\beta}C_5\,{}^{\alpha\beta}A_2 + {}^{\alpha\beta}C_1\frac{H_{1111}}{\Delta} + 4^{\alpha\beta}C_3\,{}^{\alpha\beta}A_1\right\}{}^{\alpha\beta}e_{22}. \end{aligned}$$

In the above expressions:

$$\begin{aligned} &{}^{\alpha\beta}C_1 = \sin^4{}^{\alpha\beta}\phi, \quad {}^{\alpha\beta}C_2 = \sin^3{}^{\alpha\beta}\phi\cos{}^{\alpha\beta}\phi, \quad {}^{\alpha\beta}C_3 = \sin^2{}^{\alpha\beta}\phi\cos^2{}^{\alpha\beta}\phi, \\ &{}^{\alpha\beta}C_4 = \sin{}^{\alpha\beta}\phi\cos^3{}^{\alpha\beta}\phi, \quad {}^{\alpha\beta}C_5 = \cos^4{}^{\alpha\beta}\phi. \end{aligned} \tag{5.10}$$

As discussed previously in [3], micromechanics considers it sufficient to deal with the first statistical moment of the orientation and material coefficients involved in obtaining an explicit form of the material operator ${}^{M}\mathfrak{M}$ for polycrystalline solids. Experience has shown that without invoking this assumption a large number of equations would result from which one can hardly hope to extract a solution.

To begin with, the first average quantities we wish to determine are for the orientation terms in ${}^{\alpha\beta}\mathbf{\Lambda}$ defined in (5.7). As theoretically indicated in Table 2 this can, in general, be written as:

$$\mathbf{\Lambda} = \langle {}^{\alpha\beta}\mathbf{\Lambda} \rangle = \int {}^{\alpha\beta}\mathbf{\Lambda} d\mathscr{P}^{n}. \tag{5.11}$$

However, in the context of the boundary value configuration under discussion in this paper, (5.11) ultimately reduces to a consideration of the terms

$$C_I = \langle {}^{\alpha\beta}C_I \rangle, \quad I = 1, \ldots, 5 \tag{5.12}$$

only, where the ${}^{\alpha\beta}C_I$ are defined in (5.10) and utilized in (5.9). As mentioned in Sect. 2, three particular probabilities of crystallographic grain boundary orientations are studied in order to examine the effect of the shape of the microelements on the microstress distributions discussed in Sect. 7. The three probability measures of interest are chosen to be:

$$\mathscr{P}^{\phi} = \frac{\phi}{\pi}\{H(\phi) - H(\phi - \pi)\}, \quad \mathscr{P}^{\phi} = \delta(\phi), \quad \mathscr{P}^{\phi} = \delta\left(\phi - \frac{\pi}{2}\right), \tag{5.13}$$

Table 6. Grain boundary interpretations of ΛE and $(\Lambda E)^{-1}$ for copper and aluminium at 673°K

Equation	Variable	$\mathscr{P}^{\phi} = \frac{\phi}{\pi}\{H(\phi) - H(\phi-\pi)\}$	$\mathscr{P}^{\phi} = \delta(\phi)$	$\mathscr{P}^{\phi} = \delta(\phi - \pi/2)$
(5.10)	C_1	0.375	0	1
	C_2	0	0	0
	C_3	0.125	0	0
	C_4	0	0	0
	C_5	0.375	1	0

		Copper			Aluminium		
H_{1111} dynes/cm²		36.4195×10^{11}			12.4565×10^{11}		
$\Delta = 4a$ Å		10.2			11.8		
		ϕ/π	$\delta(\phi)$	$\delta(\phi-\pi/2)$	ϕ/π	$\delta(\phi)$	$\delta(\phi-\pi/2)$
(5.16) dynes/cm²	$B_{11}(\times 10^{11})$	27.18149	36.4195	22.77456	15.17496	12.4565	15.18424
	$B_{12} = B_{21}(\times 10^{11})$	2.41554	0	0	−1.35459	0	0
	$B_{22}(\times 10^{11})$	27.18149	22.77456	36.4195	15.17496	15.18424	12.4565
(5.19) dynes/cm²	$B_{33} = 1/C_{33}(\times 10^{11})$	17.36670	19.93488	19.93488	13.07445	19.23875	19.23875
	$C_{11}(\times 10^{-13})$	3.70825	2.74578	4.39086	6.64273	8.027937	6.58578
	$C_{12} = C_{21}(\times 10^{-13})$	−0.32949	0	0	0.59296	0	0
	$C_{22}(\times 10^{-13})$	3.70825	4.39086	2.74578	6.64273	6.58578	8.027937

where H is the Heaviside step function and δ is the Dirac-delta function. The effect of this choice on the values of C_I, $I = 1, \ldots, 5$, is shown in Table 6.

The second group of quantities that we wish to average are the ${}^{\alpha\beta}A_a$ obtained from the computer simulation. Motivated by the available data and the experimental confirmation of CHAUDHARI and MATTHEWS [14] we choose for both copper and aluminium a probability measure of the form:

$$\mathscr{P}^\theta = \frac{1}{5}\{\delta(\theta-22.6)+\delta(\theta-28.1)+\delta(\theta-31.9)+\delta(\theta-36.9)+\delta(\theta-53.1)\}. \tag{5.14}$$

Using this measure the first statistical moments of ${}^{\alpha\beta}A_a$, i.e., $A_a = \langle {}^{\alpha\beta}A_a \rangle$ are obtained and expressed in Table 5. Hence, in doing so, relation (5.9) reduces to:

$$\begin{aligned}
\frac{{}^{\alpha\beta}\xi_{11}}{\Delta} &= \left(C_1 A_2 + C_5 \frac{H_{1111}}{\Delta} + 4C_3 A_1\right){}^{\alpha\beta}e_{11} + C_3\left(A_2 + \frac{H_{1111}}{\Delta} - 4A_1\right){}^{\alpha\beta}e_{22}, \\
\frac{{}^{\alpha\beta}\xi_{22}}{\Delta} &= \left(C_5 A_2 + C_1 \frac{H_{1111}}{\Delta} + 4C_3 A_1\right){}^{\alpha\beta}e_{22} + C_3\left(A_2 + \frac{H_{1111}}{\Delta} - 4A_1\right){}^{\alpha\beta}e_{11}, \\
\frac{{}^{\alpha\beta}\xi_{12}}{\Delta} &= \left\{C_3 A_2 + C_3 \frac{H_{1111}}{\Delta} + 2(C_5 - 2C_3 + C_1)A_1\right\}{}^{\alpha\beta}e_{12}.
\end{aligned} \tag{5.15}$$

Now, identifying:

$${}^{\alpha\beta}\boldsymbol{\xi} \sim \begin{bmatrix} {}^{\alpha\beta}\xi_{11} \\ {}^{\alpha\beta}\xi_{22} \\ {}^{\alpha\beta}\xi_{12} \end{bmatrix}, \qquad {}^{\alpha\beta}\mathbf{e} \sim \begin{bmatrix} {}^{\alpha\beta}e_{11} \\ {}^{\alpha\beta}e_{22} \\ {}^{\alpha\beta}e_{12} \end{bmatrix},$$

$$\mathsf{B} = \Delta \begin{bmatrix} \left(C_1 A_2 + C_5 \dfrac{H_{1111}}{\Delta} + 4C_3 A_1\right), & C_3\left(A_2 + \dfrac{H_{1111}}{\Delta} - 4A_1\right), & 0 \\ B_{21} = B_{12}, & \left(C_5 A_2 + C_1 \dfrac{H_{1111}}{\Delta} + 4C_3 A_1\right), & 0 \\ 0, & 0, & \left[C_3 A_2 + C_3 \dfrac{H_{1111}}{\Delta} + 2(C_5 - 2C_3 + C_1)A_1\right] \end{bmatrix} \tag{5.16}$$

it is seen that (5.15) may be written as:

$${}^{\alpha\beta}\boldsymbol{\xi} = \mathsf{B}\,{}^{\alpha\beta}\mathbf{e}, \tag{5.17}$$

and that it has a unique inverse:

$${}^{\alpha\beta}\mathbf{e} = \mathsf{C}\,{}^{\alpha\beta}\boldsymbol{\xi} \tag{5.18}$$

in which

$$\mathsf{C} \sim \begin{bmatrix} \dfrac{B_{22}}{B_{11}B_{22} - B_{12}^2}, & \dfrac{-B_{12}}{B_{11}B_{22} - B_{12}^2}, & 0 \\ C_{21} = C_{12}, & \dfrac{B_{11}}{B_{11}B_{22} - B_{12}^2}, & 0 \\ 0, & 0, & \dfrac{1}{B_{33}} \end{bmatrix} \tag{5.19}$$

The only variable in the above series of equations which remains to be decided is the thickness, Δ, of the grain boundary material. As discussed in [10] a good approximation to its actual value is given by:

$$\Delta = 4a, \tag{5.20}$$

where a is the lattice constant of the FCC Materials being considered.

Before turning to the actual determination of the material operator ${}^{M}\mathfrak{M}$, several interesting points should be noted. Firstly, since the setup of the problem has resulted in the Eq. (5.17) which is essentially the starting point of the plane strain problem, the matrix B identifies a particular two-dimensional interpretation of the general three-dimensional expression, $\mathbf{\Lambda E}$. Hence, when obtaining the inverse relations to B, expressed as C in (5.19) and in Table 6, the values of C do not correspond to the three-dimensional values of $(\mathbf{\Lambda E})^{-}i$ with which C is identified. As we shall see this has implications on the numerical values of ${}^{M}\mathfrak{M}$ about to be discussed. Finally, for the grain boundary orientation distributions $\mathscr{P}^{\phi} = \delta(\phi)$ and $\mathscr{P}^{\phi} = \delta\left(\phi - \frac{\pi}{2}\right)$ Eq. (5.15) or (5.17) becomes:

$$\begin{aligned} \mathscr{P}^{\phi} = \delta(\phi): \quad {}^{\alpha\beta}\boldsymbol{\xi} &= \begin{bmatrix} H_{1111} & 0 & 0 \\ 0 & A_2\Delta & 0 \\ 0 & 0 & 2A_1\Delta \end{bmatrix}{}^{\alpha\beta}\mathbf{e}, \\ \mathscr{P}^{\phi} = \delta\left(\phi - \frac{\pi}{2}\right): {}^{\alpha\beta}\boldsymbol{\xi} &= \begin{bmatrix} A_2\Delta & 0 & 0 \\ 0 & H_{1111} & 0 \\ 0 & 0 & 2A_1\Delta \end{bmatrix}{}^{\alpha\beta}\mathbf{e}, \end{aligned} \tag{5.21}$$

as expected.

6. The material operator

With reference to paper [3] and Table 2, the elastic material operator for polycrystalline solids may in general, be represented by:

$${}^{M}\mathfrak{M} = [(1-\varkappa)\mathsf{H}^{-1} + \varkappa(\mathbf{\Lambda E})^{-1}]^{-1}. \tag{6.1}$$

The term H^{-1}, representing the mechanical behaviour of single monocrystals, has already been discussed in Sect. 4 whilst $(\mathbf{\Lambda E})^{-1}$, representing the grain boundary influence, has been developed in the previous section. The only variable which remains unspecified for the present boundary value configuration is the statistical frequency of grain boundary influenced material, $\varkappa$. $\varkappa$ is a function of the distribution of the sizes of microelements, the value of Δ, the grain boundary orientation probability measure and the boundary value configuration being investigated. Although various expressions for $\varkappa$, based upon reasoning related to geometric properties and the first statistical moment of the geometric parameters involved, can easily be envisaged, results are presented for copper and aluminium for the three chosen values of $\varkappa$ as follows:

$$\varkappa = 0.01, \quad 0.05, \quad 0.2. \tag{6.2}$$

Table 7. ${}^{M}\mathfrak{m}$ **for copper and aluminium**

		Copper dynes/cm²				Aluminium dynes/cm²			
$\varkappa$	$\mathscr{P}\phi$	${}^{M}\mathfrak{m}_{1111}$ ($\times 10^{11}$)	${}^{M}\mathfrak{m}_{1122}$ ($\times 10^{11}$)	${}^{M}\mathfrak{m}_{2222}$ ($\times 10^{11}$)	${}^{M}\mathfrak{m}_{1212}$ ($\times 10^{11}$)	${}^{M}\mathfrak{m}_{1111}$ ($\times 10^{11}$)	${}^{M}\mathfrak{m}_{1122}$ ($\times 10^{11}$)	${}^{M}\mathfrak{m}_{2222}$ ($\times 10^{11}$)	${}^{M}\mathfrak{m}_{1212}$ ($\times 10^{11}$)
0.01	ϕ/π	27.97337	9.02489	27.97337	18.88688	8.72752	3.00817	8.72752	5.71413
	$\delta(\phi)$	28.02662	9.00355	2.72802	18.91338	8.72014	3.00973	8.72981	5.72214
	$\delta(\phi-\pi/2)$	27.2802	9.00355	28.02662	18.91338	8.72981	3.00973	8.72014	5.72214
0.05	ϕ/π	27.8791	8.74906	27.8791	18.82031	8.84111	2.96653	8.84111	5.84712
	$\delta(\phi)$	28.15069	8.64361	27.5737	18.95262	8.80299	2.97488	8.85281	5.88932
	$\delta(\phi-\pi/2)$	27.5737	8.64361	28.15069	18.95262	8.85281	2.97488	8.80299	5.88932
0.2	ϕ/π	27.57345	7.73043	27.57345	18.57483	9.3129	2.77266	9.3129	6.40627
	$\delta(\phi)$	28.74221	7.32287	26.42022	19.10122	9.13914	2.18564	9.36308	6.61395
	$\delta(\phi-\pi/2)$	26.42022	7.32287	28.74221	19.10122	9.36308	2.81564	9.13914	6.61395

Basically, without including the influence of the shape and orientation of microelements, large values of $\varkappa$ represent large values of Δ and/or smaller sizes of the individual grains. With the choice of (6.2) the information contained in Tables 4 and 6 may be combined to give the final quantitative values of ${}^{M}\mathfrak{M}$, listed in Table 7, for the effective elastic response of randomly oriented polycrystalline solids in tension. It is to be noted, however, that ${}^{M}\mathfrak{M}$ is an operator and not simply the numerical reciprocal of each individual ${}^{M}\mathfrak{M}^{-1}$ term and that it corresponds to the inverse of a two-dimensional operator, not a three-dimensional one, for the reason discussed at the end of the previous section. The different strengths of copper and aluminium as a function of crystal shape, orientation and size in Table 7 is a clear validation of the micromechanic approach to the description of the mechanical response of polycrystalline solids.

7. Microstress distributions

The specific information concerning the microstrain distributions, as discussed, along with their limitations, in Sect. 3, and the material properties, as presented in Sect. 6, can now be combined to give an estimate of the microstress distributions for this particular boundary value configuration and for these specific materials. These microstress distributions are obtained from the general expressions, whose derivation is discussed in [3]:

$$\mathscr{P}^{\xi} = {}^{M}\mathfrak{M}\,\mathscr{P}^{e}, \tag{7.1}$$

$$\langle \boldsymbol{\xi} \rangle = {}^{M}\mathfrak{M}\langle \mathbf{e} \rangle, \tag{7.2}$$

$$\mathsf{V}\xi = {}^{M}\mathfrak{M}\,{}^{M}\mathfrak{M}^{T}\mathsf{V}_{e}, \tag{7.3}$$

where $\langle \cdot \rangle$ indicates a first moment and V the variance of the subscripted parameter. Since micromechanics concerns itself with the first and second statistical moments of the parameters involved and assumes all distributions to be Gaussian, the relations (7.2) and (7.3) are sufficient to specify the microstresses inherent in the material under review. In the context of the present boundary value configuration and utilizing the values listed in Tables 3 and 7, the Eqs. (7.2) and (7.3) reduce, respectively, to:

$$\langle \xi_{11} \rangle = {}^{M}\mathfrak{M}_{1111}\langle e_{11} \rangle, \quad \langle \xi_{22} \rangle = {}^{M}\mathfrak{M}_{1122}\langle e_{11} \rangle, \quad \langle \xi_{12} \rangle = 0, \tag{7.4}$$

and:

$$\begin{aligned} \sigma_{\xi_{11}} &= \sqrt{V_{\xi_{11}}} = ({}^{M}\mathfrak{M}^{2}_{1111} V_{e_{11}} + {}^{M}\mathfrak{M}^{2}_{1122} V_{e_{22}})^{1/2}, \\ \sigma_{\xi_{22}} &= \sqrt{V_{\xi_{22}}} = ({}^{M}\mathfrak{M}^{2}_{1122} V_{e_{11}} + {}^{M}\mathfrak{M}^{2}_{2222} V_{e_{22}})^{1/2}, \\ \sigma_{\xi_{12}} &= \sqrt{V_{\xi_{12}}} = ({}^{M}\mathfrak{M}^{2}_{1212} V_{e_{12}})^{1/2}. \end{aligned} \tag{7.5}$$

The values of $\langle \boldsymbol{\xi} \rangle$ and σ_{ξ}, where σ is the standard deviation, are listed in Table 8. There is, of course, no method of verifying these results either in terms of the means or in terms of the variances.

Sets of readings, extracted from Table 8, are illustrated in Fig. 3 for the material parameters shown. The general characteristics of these normally distributed microstress densities are primarily due to the strain histograms developed in Sect. 3. For this reason

Table 8. Microstress means and variances

		Copper						Aluminium					
		(dynes/cm² × 10⁹)						(dynes/cm² × 10⁹)					
$\varkappa$	ϕ	$\langle\xi_{11}\rangle$	$\sigma_{\xi_{11}}$	$\langle\xi_{22}\rangle$	$\sigma_{\xi_{22}}$	$\langle\xi_{12}\rangle$	$\sigma_{\xi_{12}}$	$\langle\xi_{11}\rangle$	$\sigma_{\xi_{11}}$	$\langle\xi_{22}\rangle$	$\sigma_{\xi_{22}}$	$\langle\xi_{12}\rangle$	$\sigma_{\xi_{12}}$
0.01	ϕ/π	1.2448	0.6032	0.4016	0.7222	0.0	0.5666	0.3884	0.1901	0.1339	0.2263	0.0	0.1714
	$\delta(\phi)$	1.2472	0.6040	0.4007	0.7054	0.0	0.5674	0.3880	0.1899	0.1339	0.2264	0.0	0.1716
	$\delta\left(\phi\frac{\pi}{2}\right)$	1.2140	0.5902	0.4007	0.7234	0.0	0.5674	0.3885	0.1901	0.1339	0.2262	0.0	0.1716
0.05	ϕ/π	1.2406	0.5989	0.3893	0.7186	0.0	0.5645	0.3934	0.1917	0.1320	0.2289	0.0	0.1754
	$\delta(\phi)$	1.2527	0.6030	0.3846	0.7107	0.0	0.5686	0.3917	0.1911	0.1324	0.2292	0.0	0.1767
	$\delta\left(\phi-\frac{\pi}{2}\right)$	1.2270	0.5923	0.3846	0.7247	0.0	0.5686	0.3940	0.1920	0.1324	0.2280	0.0	0.1767
0.2	ϕ/π	1.2270	0.5843	0.3440	0.7065	0.0	0.5572	0.4144	0.1987	0.1234	0.2393	0.0	0.1922
	$\delta(\phi)$	1.2790	0.6033	0.3259	0.6765	0.0	0.5730	0.4067	0.1959	0.1253	0.2408	0.0	0.1984
	$\delta\left(\phi-\frac{\pi}{2}\right)$	1.1757	0.5592	0.3259	0.7333	0.0	0.5730	0.4166	0.2000	0.1253	0.2353	0.0	0.1984

no emphasis is placed on the actual numerical values obtained. Qualitatively, it is immediately noticed, however, that while there is a positive average stress in both copper and aluminium the possibility still exists for stresses to be compressive, an observation similar to that made on thermodynamic grounds by KESTIN [17]. At the other extreme,

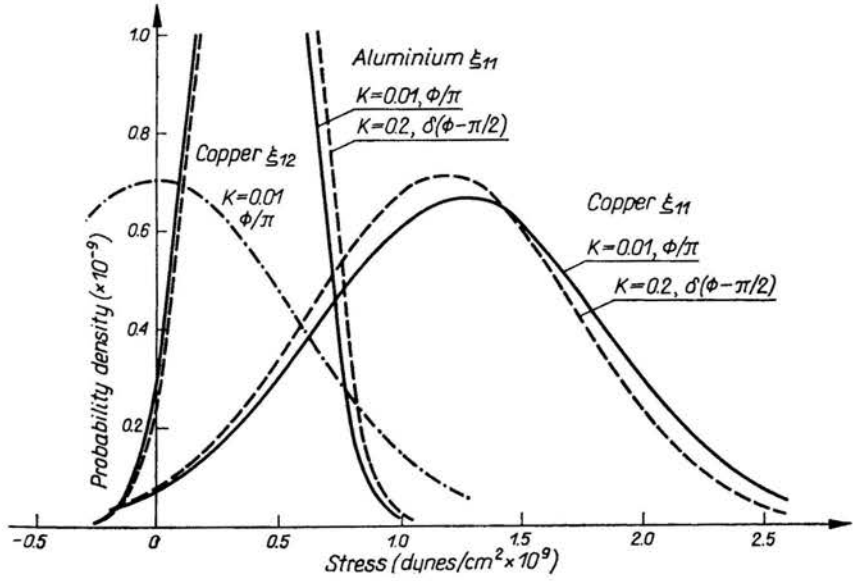

FIG. 3. Examples of microstress distributions for copper and aluminium.

microstresses exist in a polycrystalline solid which may be considerably higher than that of the mean stress, a fact of interest not only to researchers in probabilistic solid mechanics but also to the practicing stress analyst. The second fact which may be observed is that the effect of grain boundaries and their orientation distributions is not pronounced. This is due to the elastic grain boundary responses, as developed in Sect. 5, not being radically different from the bulk material response. This is expected to reverse itself when irreversible responses of grain boundaries are included, at a future date, in the analysis of time dependent responses of structured materials. One aspect which does not come out of the results is the importance of microstress gradients obtained from a correlation formulation as discussed in [1, 4 and 8]. Hence, both the table and figure clearly illustrate the usefulness of the micromechanics approach.

Running the possible risk of being repetitive, any structured solid is amenable to a micromechanic approach. The accumulation, however, of the necessary microscopic information concerning the material in question is, as has been amply summarized in this paper, a time consuming and often frustrating requirement of the theory if specific results are to be presented. It is not just sufficient to develop mechanical response theories from abstract mathematical principles. Such theories must be verified both experimentally and numerically by their proponents if they are ever to be accepted. This paper represents our first attempt at carrying out such a validation of micromechanics. Table 8 infers

that the philosophy behind and principles laid down in micromechanics over the last decade are worthwhile developing further into fields concerned with different materials, configurations and mechanical responses.

Acknowledgments

The authors greatly appreciate the financial support given to them by the National Research Council of Canada under the grants A7525 and A2890 which made this research possible.

References

1. D. R. AXELRAD, J. W. PROVAN, *Probabilistic micromechanics of structured solids* [in Polish] in "Teorie statystyczne w ciałach stałych, cieczach i gazach", Polska Akademia Nauk, 5–80, 1974.
2. D. R. AXELRAD, *Micromechanics of solids*, Polish Academy of Sciences, Warsaw and Elsevier Publ. Co., Amsterdam (Holland) to be published (1975–76).
3. J. W. PROVAN, D. R. AXELRAD, *Probabilistic micromechanics of inhomogeneous solids*, Reviews on the Deformation Behaviour of Materials (to be published).
4. D. R. AXELRAD, J. W. PROVAN, *Deformation theory of elastic polycrystalline materials*, Arch. Mech. Stos., **25**, 811, 1973.
5. D. R. AXELRAD, J. W. PROVAN, S. BASU, *Analysis of the semi-group property and the constitutive relations of structured solids*, Proceedings of Conf. on Symmetry in Mechanics, Calgary, Aug. 1974.
6. D. R. AXELRAD, J. KALOUSEK, *Measurement of microdeformations by holographic X-Ray diffraction*, Experimental Mechanics in Research and Development, Study No. 9, ed. J. T. PINDERA *et al.*, University of Waterloo Press, 1973.
7. J. KALOUSEK, *Experimental Investigation of the Deformation of Structured Media*, Ph. D. Thesis, McGill University, 1973.
8. D. R. AXELRAD, J. W. PROVAN, S. el HELBAWI, *Dislocation effects in elastic structured solids*, Arch. Mech. Stos., **25**, 801, 1973.
9. O. A. BAMIRO, J. W. PROVAN, *Grain boundary entropies and free energies of copper, gold and aluminium*, Surface Science (submitted for publication).
10. J. W. PROVAN, O. A. BAMIRO, *On elastic grain boundary responses in copper and aluminium*, Surface Science (submitted for publication).
11. D. R. AXELRAD, *Micromechanics of discrete systems*, Arch. Mech. Stos. (to be published).
12. J. P. HIRTH, J. LOTHE, *Theory of Dislocations*, McGraw-Hill, 1968.
13. A. V. GRANATO, *Internal friction studies of dislocation motion*, in "Dislocation Dynamics", eds. A. R. ROSENFIELD, G. I. HAHN, A. L. BEMENT and R. I. JAFFEE, 117–157, McGraw-Hill, 1968.
14. P. CHAUDHARI, J. W. MATTHEWS, *Coincidence first boundaries between crystalline smoke particles*, J. Appl. Phys., **42**, 3063, 1971.
15. A. T. Di BENEDETTO, *The Structure and Properties of Materials*, McGraw-Hill, 295, New York, 1967.
16. G. Y. CHIN, W. F. HOSFORD, W. A. BACHOFEN, *Ductile fracture of aluminium*, Trans. ASME, **230**, 437, 1964.
17. J. KESTIN, *On the application of the principles of thermodynamics to strained solid materials*, in "Irreversible Aspects of Continuum Mechanics...", eds. H. Parkus and L. T. Sedov, 177–212, Springer-Verlag, 1968.

MICROMECHANICS OF SOLIDS LABORATORY
McGILL UNIVERSITY, MONTREAL, CANADA.